

Connection stiffness and natural frequency of DuraGal lightweight floor systems

X.L. Zhao[†], G. Taplin[‡] and M. Alikhail^{‡†}

Department of Civil Engineering, Monash University, Clayton, VIC 3168, Australia

(Received January 5, 2001, Revised September 16, 2002, Accepted February 6, 2003)

Abstract. This paper reports a series of component tests on a lightweight floor system and a method to predict the natural frequency of the floor using a frame analysis program. Full-scale floor tests are also briefly described. DuraGal steel Rectangular Hollow Sections (in-line galvanised RHS) are used as joists, bearers and piers in DuraGal lightweight floor systems. A structural grade particleboard is used as decking. Connection stiffness between different components (bearer, joist, pier and floor decking) was determined. A 40% composite action was achieved between the RHS joist and the particleboard. Both 2D and 3D models were developed to study the effect of connection stiffness on predicting the natural frequency of DuraGal lightweight floor systems. It has been found that the degree of shear connection between the bearer and the joist has a significant influence on the floor natural frequency. The predicted natural frequencies are compared with measured values from full scale floor testing.

Key words: floor system; steel hollow sections; rotational stiffness; natural frequency.

1. Introduction

1.1 DuraGal floor systems

A lightweight steel floor system was developed by BHP Structural and Pipeline Products (now OneSteel) utilising DuraGal steel rectangular hollow section (RHS) piers, bearers and joists (Alikhail *et al.* 1998). A schematic view of the floor system is presented in Fig. 1. The floor system is designed for easy erection, and is assembled using a range of standard components and connectors. The height of the piers can be adjusted using an adjustable connection (see Fig. 2) to allow accurate leveling in floor construction. The DuraGal steel rectangular hollow sections are manufactured using cold-formed process with in-line galvanising (Zhao and Mahendran 1998). A structural grade particleboard (Structaflor) was used as floor decking. This flat pressed, class 1 particleboard decking complies with the Australian Standard AS1859 (SAA 1980).

1.2 Natural frequency and connection stiffness

“Annoying vibration” is a serviceability problem in all floor systems. The first natural frequency

[†] Professor

[‡] Senior Lecturer

^{‡†} PhD Student

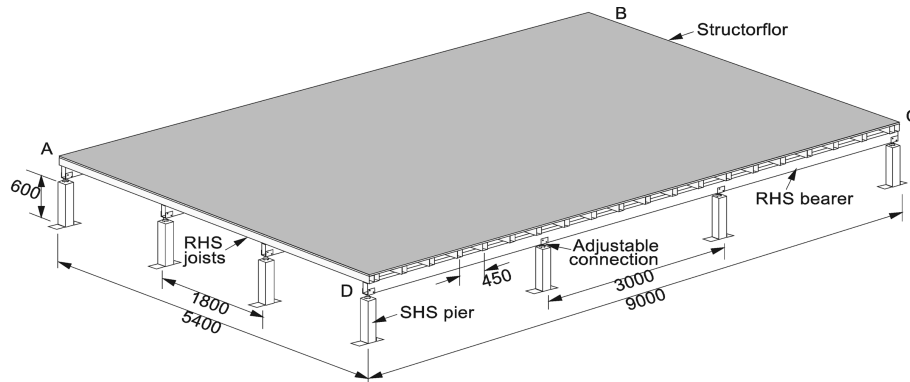


Fig. 1 DuraGal lightweight floor system

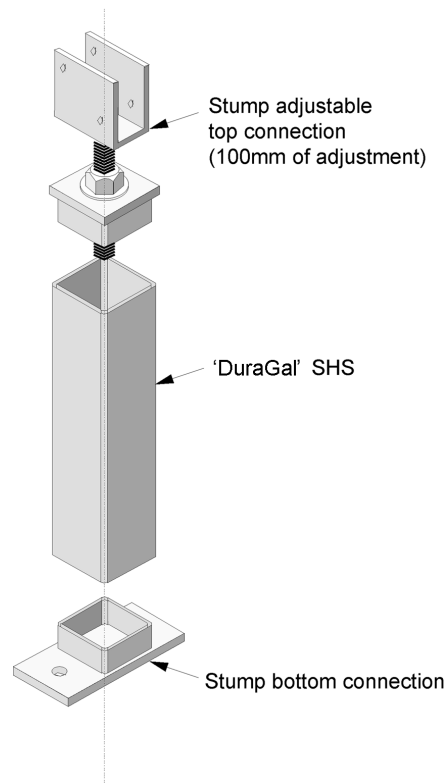


Fig. 2 Adjustable connection

and damping ratio are two important parameters when assessing whether a floor has annoying vibration or not (Lenzen 1966, Wiss and Parmelee 1974, Allen and Rainer 1976, Ohlsson 1982, Murray 1991, Onysko 1995, Alikhail *et al.* 1998, 1999). Damping ratios were recommended as 2% to 6% for DuraGal floors at different stages of construction (Alikhail *et al.* 2000). There were several approaches to predict the natural frequency of a floor:

Table 1 Experimental natural frequencies

Stage	Construction Details	Fundamental Frequency (Hz)
1	Bare floor	18.9
2	Timber framed walls were built on top of the bearers	19.1
3	A ceiling was constructed supported on the timber-framed walls, using similar materials and construction to the floor. Lumped masses were distributed on the ceiling, placed directly over the walls, to increase the average mass of ceiling plus lumped masses to 40 kg/m ² . This simulated the mass of a metal deck roof.	22.2
4	The lumped masses were increased so that the average mass of ceiling plus lumped masses was 90 kg/m ² . This simulated the mass of a tile roof.	22.8

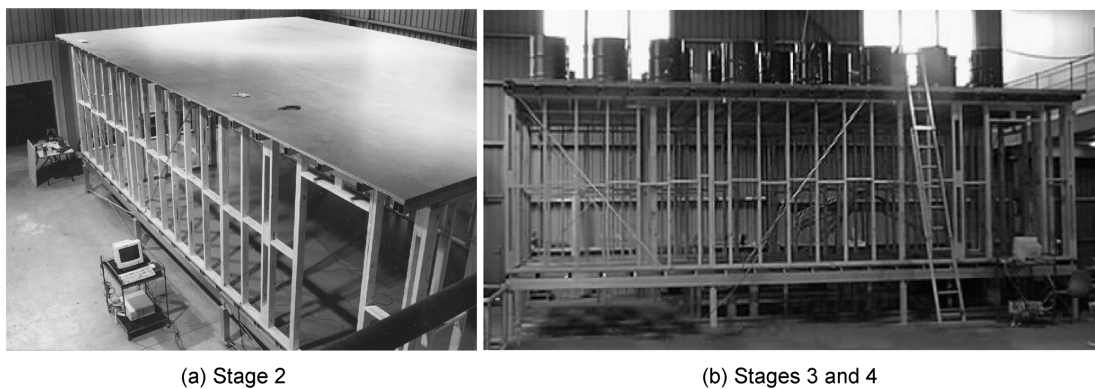


Fig. 3 Construction Stages, (a) Stage 2, (b) Stages 3 and 4

- Finite element method as reported in Alikhail *et al.* (2000) and Couchman *et al.* (1999).
- Classical stiffened plate theory as reported by Alisjahbana *et al.* (2000) which utilised the techniques of separation of variables to solve partial differential equations (Alisjahbana 2000).
- Energy method as reported by Smith and Chui (1988).

The above methods either require a finite element program or a solution to partial differential equations, which often is complicated for structural engineers. There is a need to explore a relatively simple method to predict the natural frequency of floors. As we know frame analysis programs are commonly used by structural engineers in design of structures. This paper aims to predict the natural frequency of DuraGal lightweight floor systems using SpaceGass (ITS 1998), a readily available frame analysis program in Australia. There are many similar programs based on structural frame analysis available in other countries.

The connections between the various floor components (bearer, joist, pier and floor decking) may have a significant influence on the natural frequency of DuraGal lightweight floor systems. The natural frequency of a typical floor system at four different construction stages (see Table 1, Figs. 1 and 3) was determined from full-scale floor testing. Six types of component tests on lightweight floor systems were carried out to measure the connection stiffness. Composite actions between steel RHS joist and floor decking are determined by testing bare RHS beams and part of floors

containing RHS joints and floor decking. Different models (both 2D and 3D) were developed to study the effect of connection stiffness on predicting the natural frequency of DuraGal lightweight floor systems. The predicted values are compared with the experimental ones obtained in the full-scale floor testing. The paper shows that the natural frequency increases as the construction stage progresses.

2. Full scale floor testing

Tests were carried out on a series of full-scale DuraGal lightweight floors in the Civil Engineering Laboratory at Monash University. The tests included determination of static deflections under a point load on the floor and dynamic properties (natural frequency and damping ratios) for floors at four different stages of construction. Subjective evaluations were also conducted to assess if the floor produces annoying vibration.

A DuraGal floor of rectangular shape (A B C D) with dimension 9000 mm by 5400 mm was constructed in the Civil Engineering Laboratory at Monash University. The floor had a joist-span of 1800 mm; a joist spacing of 450 mm and a bearer span of 3000 mm as shown in Fig. 1. To carry out the measurements, a sledgehammer with a built-in force transducer was used to excite the floor. The vibration in the floor was measured using seven accelerometers connected to a multi-channel data acquisition system. The Experimental Modal Analysis (EMA) technique was used to collect a comprehensive set of Frequency Response Functions (FRFs) at a number of points on the floor. Details of the test program were reported in Alikhail *et al.* (1999). Only the results of natural frequency are summarised in Table 1 of this paper for comparison purpose. The different stages are shown in Fig. 1 for Stage 1, Fig. 3(a) for Stage 2 and Fig. 3(b) for Stages 3 and 4. The values of 40 kg/m² and 90 kg/m² for Stages 3 and 4, as listed in Table 1, are corresponding to the loads specified in the Australian Domestic Construction Manual (Dawkins and Cusack 1993) for sheet metal roof and tile roof respectively. It is interesting to note that the addition of the lumped masses (Stages 3 and 4) increased the frequency of vibration, which is contrary to normal expectation. This will be further discussed later in Section 4.5.

3. Component tests

3.1 Types of tests

There are a number of connections between the components in DuraGal lightweight floor systems, i.e., the adjustable connection between the pier and the bearer (see Figs. 4d, e), the connection between the bearer and the joist (see Fig. 4b), the connection between the joist and the particleboard (see Fig. 1c). The sizes for pier, bearer and joist are RHS 90 × 90 × 2, RHS 150 × 50 × 2 and RHS 100 × 50 × 2 mm respectively. The thickness of the particleboard is 19 mm.

In order to establish a reliable analytical model of the floor behaviour, it is necessary to have data on the stiffness of these connections. For this reason an experimental program was carried out comprising:

Type 1 test - testing of a simply supported joist to act as a reference test (see Fig. 4a).

Type 2 test - testing of a single span joist which was connected to fixed bearers - to measure the

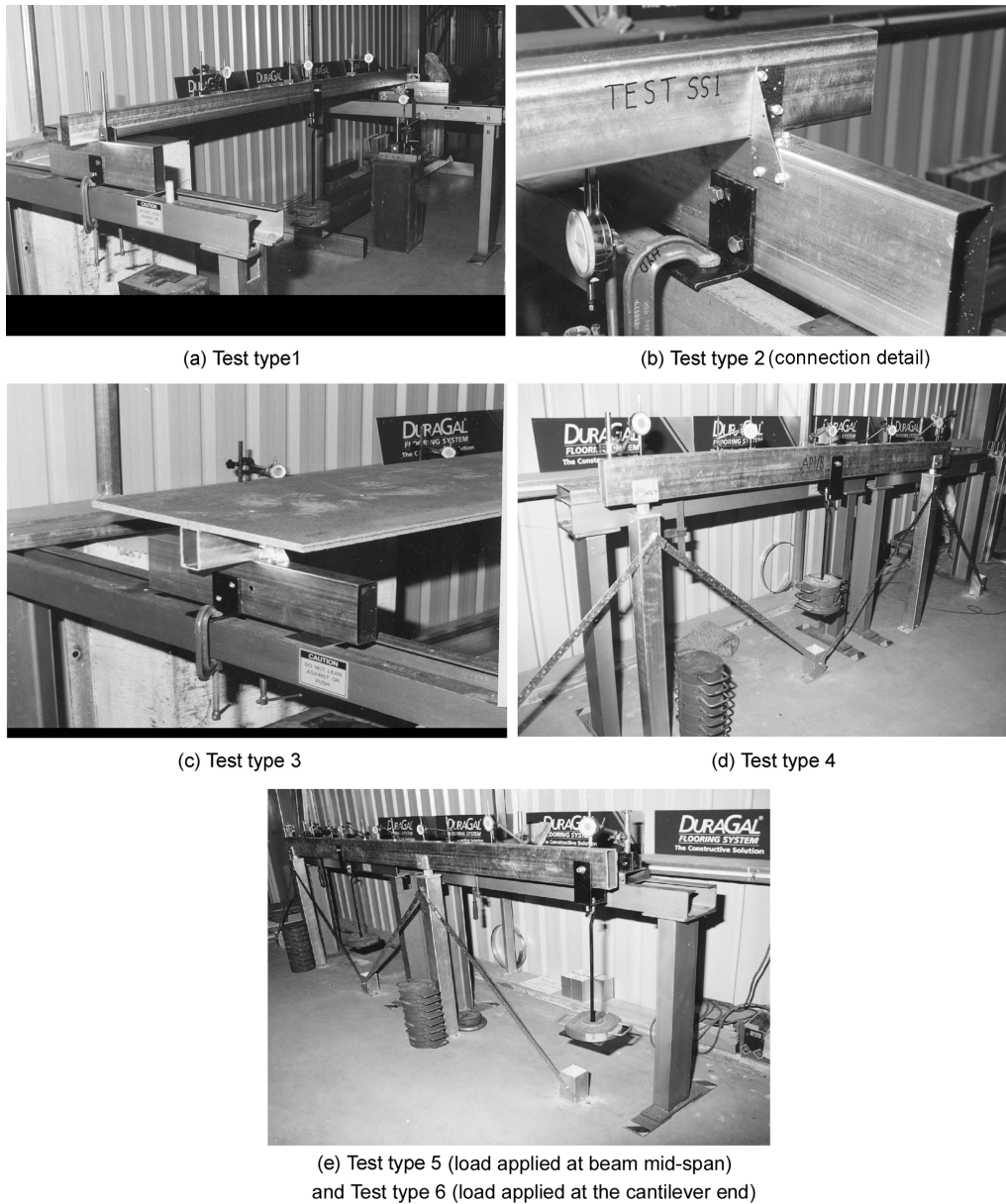


Fig. 4 Component tests

bending stiffness of the joist to bearer connection (see Fig. 4b).

Type 3 test - testing of a single span composite joist (comprising a joist and a 600 mm wide strip of particleboard connected to the top surface) which was connected to fixed bearers - to measure the bending stiffness of the composite joist/flooring section (see Fig. 4c). The value of 600 mm corresponds to the typical joist spacing used in construction.

Type 4 test - testing of a single span bearer supported at each end on a pier - to measure the bending stiffness between the pier and the bearer (see Fig. 4d).

Table 2 Results of test Types 1, 2, and 3

Load P (N) (1)	$\Delta_{midspan}$ (Theory) (mm) (2)	$P/\Delta_{midspan}$ (theory) (N/mm) (3)	$\Delta_{midspan}$ (Type 1) (mm) (4)	$P/\Delta_{midspan}$ (Type 1) (N/mm) (5)	$\Delta_{midspan}$ (Type 2) (mm) (6)	$P/\Delta_{midspan}$ (Type 2) (N/mm) (7)	$\Delta_{midspan}$ (Type 3) (mm) (8)	$P/\Delta_{midspan}$ (Type 3) (N/mm) (9)	Ratio (column 9 /column 7) (10)
0	0	--	0	--	0	--	0	--	--
38	0.140	273	0.105	364	0.103	373	0.045	849	2.28
136	0.510	267	0.450	303	0.403	338	0.265	514	1.52
234	0.880	266	0.785	298	0.723	324	0.505	464	1.43
332	1.250	266	1.115	298	1.065	312	0.745	446	1.43
430	1.610	267	1.470	293	1.395	308	0.965	446	1.45
528	1.980	267	1.800	293	1.725	306	1.205	438	1.43
626	2.350	266	2.150	291	2.050	305	1.465	427	1.40
724	2.720	266	2.490	291	2.388	303	1.725	420	1.38
822	3.090	266	2.830	291	2.693	305	2.005	410	1.34
920	3.450	267	3.160	291	3.030	304	2.290	402	1.32
1018	3.820	267	3.500	291	3.350	304	2.570	396	1.30

Table 3 Rotational stiffness ($C_{Bearer-Pier}$) for bearer and pier connection

Test Type	Loading position	Adjusted height on the left (mm)	Adjusted height on the right (mm)	Rotational Stiffness $C_{Bearer-Pier}$ (kNm/rads)
Type 4A	Midspan	0	0	48.5
Type 4B	Midspan	0	50	41.3
Type 4C	Midspan	50	50	34.6
Type 5A	Midspan	0	0	51.0
Type 5B	Midspan	50	50	33.2
Type 6A	Cantilever	0	0	43.9
Type 6B	Cantilever	0	50	37.1
Type 6C	Cantilever	50	50	29.6
Mean	--	--	--	40.0
COV	--	--	--	0.177

Type 5 and Type 6 tests - testing of a single span bearer with an extension of a cantilever - to measure the bending stiffness between the pier and the bearer (see Fig. 4e).

Three slightly different types of tests (Types 4, 5 and 6) were conducted in order to get the average value of rotational stiffness between pier and bearers under 3 different conditions.

3.2 Test set up

The test set up is shown in Figs. 1(a) to (e). The span length of the test beam was the same (3 meters) for test Types 1, 2 and 3. The locations of the dial gauges are the same for test Types 1, 2 and 3, i.e., every 750 mm apart. The span length for test Types 4, 5 and 6 was 2 meters. Dial gauges were located every 500 mm along the beam for test Types 4, 5 and 6. The extended

cantilever in the test Types 5 and 6 was 1,300 mm long. Three combinations of the adjustable height at both left and right piers were used as listed in Table 3.

The load was applied at the mid-span of the test beam for test Types 1, 2, 3, 4 and 5. The loading location for test Type 6 was near the end of the cantilever. The distance between the loading point and the support on the right is 1,200 mm. A loading device was made to transfer a balanced vertical load to the beam without affecting the section properties and behaviour of the beam. The loading device was connected to a test beam with a bolt which passes through the neutral axis of the beam. The hanger is simply hooked onto a U-bolt which is attached to the loading device. The loading device was similar to that used by Zhao *et al.* (1995).

3.3 Test results

Load deflection plots for test Types 1, 2 and 3 are presented in Fig. 5, together with the theoretical values for simply supported end conditions calculated using the nominal cross section

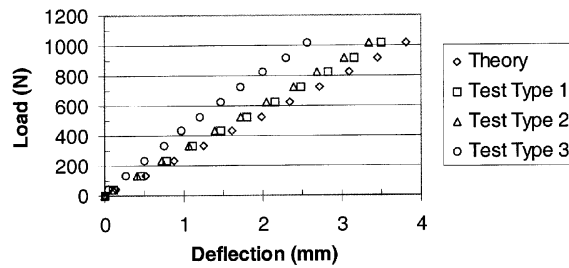


Fig. 5 Load versus midspan deflection curves (Types 1, 2 and 3)

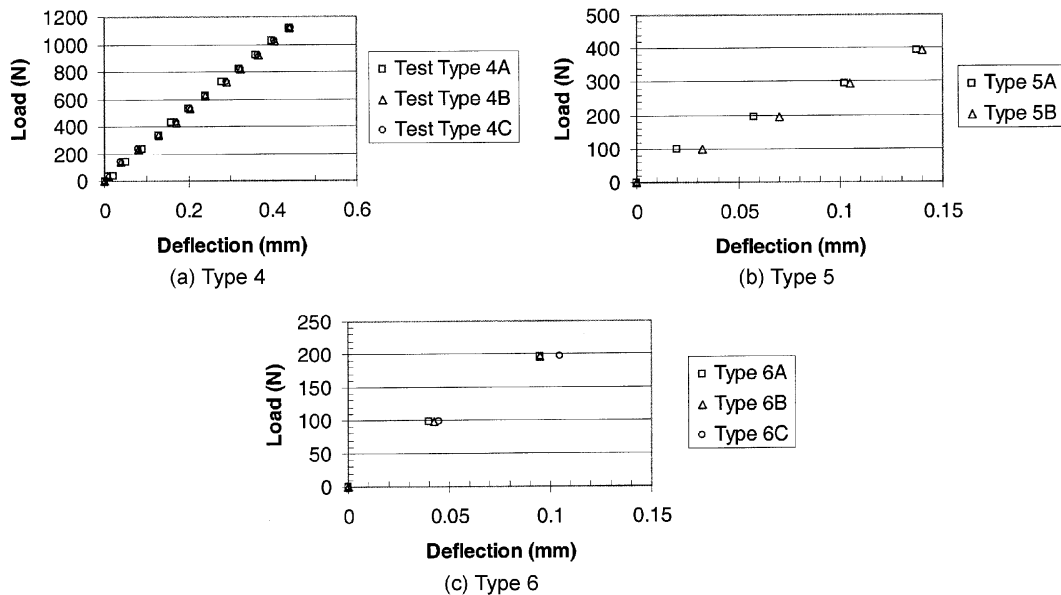


Fig. 6 Load versus midspan deflection curves, (a) Type 4, (b) Type 5 and (c) Type 6

dimensions and a value of 200,000 MPa for the elastic modulus. As expected, the stiffness increases from test Type 1 to 2 to 3.

Load deflection plots are presented in Fig. 6(a) for test Type 4, Fig. 6(b) for test Type 5 and Fig. 6(c) for test Type 6. From Fig. 6 it seems that a slightly larger deflection was obtained for connections with larger adjustable height at both ends.

4. Connection stiffness

4.1 Composite action

The detailed results of test Types 1, 2, and 3 are presented in Table 2 where the stiffness ($P/\Delta_{midspan}$) is also shown. It can be seen that the stiffness increases from Types 1 to 2 to 3. The ratio of the stiffness for Type 3 to that for Type 2 gives an indication of the composite action. The larger values of the ratio (column 10, Table 2) at lower load level may be due to the fact that the

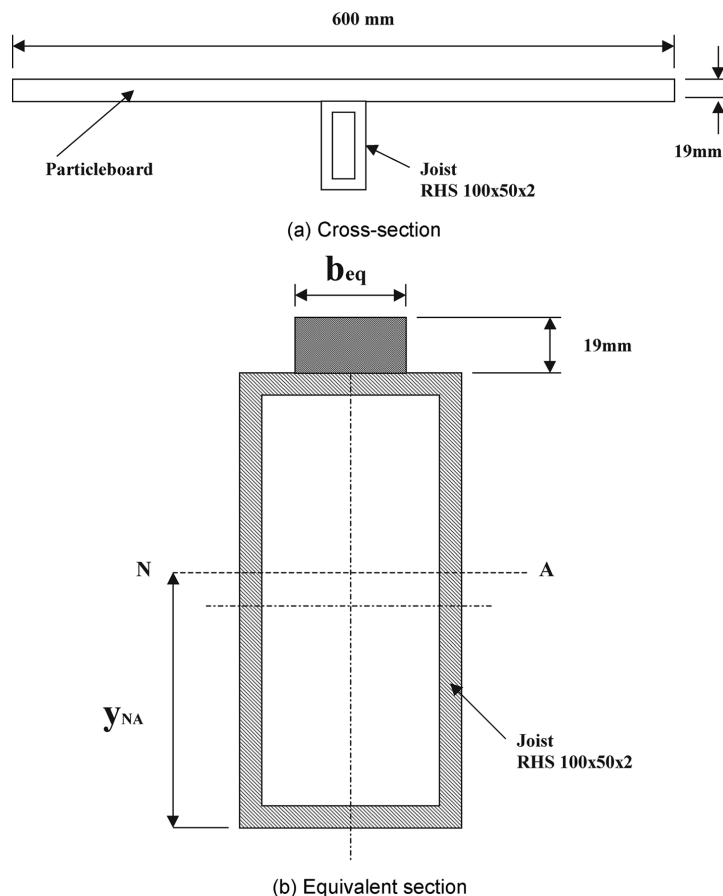


Fig. 7 Connection between joist and particleboard

deflection for Type 3 at lower loads is very small. This made the ratio more sensitive at the lower load range, e.g., below 136 N. This composite action with flooring increases the joist section stiffness around 40% (between 30% and 50%). This value is similar to that obtained by Couchman *et al.* (1999) for steel-board composite floors where light gauge channel sections are used as joists. Fig. 7(a) shows a cross-section of the Type 3 specimen. Fig. 7(b) shows the equivalent section if steel Young's modulus is used. The equivalent width (b_{eq}) for the particleboard can be calculated as:

$$b_{eq} = \left(\frac{E_{board}}{E_{steel}} \right) \cdot 600$$

The new neutral axis position (y_{NA}) can be determined for the section in Fig. 7(b). Then the equivalent second moment of area I_{eq} can be obtained accordingly. After several iterations, an effective elastic modulus for the flooring material (E_{board}) can be obtained as 1,850 MPa to achieve a 40% increase in bending stiffness, i.e.,

$$EI_{eq} = (EI)_{composite} = 1.4 \cdot (EI)_{joist} = 1.4 \cdot 200,000 \cdot 0.75 \cdot 10^6 = 2.1 \cdot 10^{11} \text{ Nmm}^2$$

4.2 Rotational stiffness between joist and bearer

For test Type 2 set up, the deflection at mid-span ($\Delta_{midspan}$) can be expressed as

$$\Delta_{midspan} = \frac{P \cdot L^3}{48 \cdot E \cdot I} - \frac{M_o L^2}{8 \cdot E \cdot I} \quad (1)$$

where P is the applied load at midspan, M_o is the moment at each end of the beam, E is the Young's modulus of elasticity, I is the second moment of area of the joist and L is the span of the beam.

The rotation angle of the beam can be estimated as:

$$\theta = \tan^{-1} \left[\frac{\Delta_{quarter-span}}{L/4} \right] \quad (2)$$

where $\Delta_{quarter-span}$ is the deflection at the quarter span of the beam.

The rotational stiffness between joist and bearer ($C_{joist-bearer}$) can be obtained by Eq. (3):

$$C_{joist-bearer} = \frac{M_o}{\theta} \quad (3)$$

in which, θ is determined using Eq. (2). M_o is derived from simply rearranging Eq. (1), i.e., moving the term $\Delta_{midspan}$ to the right and moving the term $M_o L^2/8EI$ to the left, then multiply both sides by $8EI/L^2$:

$$M_o = \frac{8 \cdot E \cdot I \cdot \left[\frac{P \cdot L^3}{48 \cdot E \cdot I} - \Delta_{midspan} \right]}{L^2} = \frac{P \cdot L}{6} - \frac{8 \cdot E \cdot I \cdot \Delta_{midspan}}{L^2} \quad (4)$$

Slightly different values of rotational stiffness could be obtained at different load level especially at a very low load level when the deflection was very small, which made the calculation sensitive to the deflection measurement and any possible gap in the system. The variation becomes much less when the load increases. The rotational stiffness in this paper is determined at the largest load of 1018 N when the beam is more settled. The given parameters are summarised below:

$$\begin{aligned} P &= 1018 \text{ N} \\ E &= 200,000 \text{ MPa} \\ I &= 0.75 \times 10^6 \text{ mm}^4 \text{ (for the joist RHS } 100 \times 50 \times 2 \text{ about its major axis)} \\ \Delta_{\text{midspan}} &= 3.35 \text{ mm} \\ \Delta_{\text{quarter-span}} &= 2.2 \text{ mm} \\ L &= 3000 \text{ mm} \end{aligned}$$

The rotation angle can be determined using Eq. (2) as:

$$\theta = \tan^{-1} \left[\frac{\Delta_{\text{quarter-span}}}{L/4} \right] = \tan^{-1} \left[\frac{2.2}{3000/4} \right] = 0.00292 \text{ rads}$$

The end moment M_o can be determined using Eq. (4) as:

$$M_o = \frac{P \cdot L}{6} - \frac{8 \cdot E \cdot I \cdot \Delta_{\text{midspan}}}{L^2} = \frac{1018 \cdot 3000}{6} - \frac{8 \cdot 200,000 \cdot 0.75 \cdot 10^6 \cdot 3.35}{3000^2} = 0.0624 \text{ kNm}$$

The rotational stiffness ($C_{\text{joist-bearer}}$) can be determined using Eq. (3) as

$$C_{\text{joist-bearer}} = \frac{M_o}{\theta} = \frac{0.0624}{0.00292} = 21.4 \text{ kNm/rads}$$

4.3 Rotational stiffness between bearer and pier

For test Types 4 and 5 the rotational stiffness between bearer and pier ($C_{\text{bearer-pier}}$) can be determined using the same formulae (Eqs. (2), (3), (4)) derived in Section 4.2 with the following properties:

$$\begin{aligned} E &= 200,000 \text{ MPa} \\ I &= 2.08 \times 10^6 \text{ mm}^4 \text{ (for the bearer RHS } 150 \times 50 \times 2 \text{ about its major axis)} \\ L &= 2000 \text{ mm} \end{aligned}$$

As mentioned before, slightly different values of rotational stiffness will be obtained at different load level. The rotational stiffness in this paper is determined at the largest load in the test when the beam is more settled as explained in Section 4.2. A summary of the calculated rotational stiffness is given in Table 3.

For test Type 6 set up, the deflection at mid-span (Δ_{midspan}) is similar to Eq. (1) and can be expressed as

$$\Delta_{\text{midspan}} = \frac{P \cdot a \cdot L^2}{48 \cdot E \cdot I} - \frac{M_o L^2}{8 \cdot E \cdot I} \quad (5)$$

where a is the distance between the loading point and the support on the right, which is 1,200 mm. Therefore the moment M_o is:

$$M_o = \frac{8 \cdot E \cdot I \cdot \left[\frac{P \cdot a \cdot L^2}{48 \cdot E \cdot I} - \Delta_{midspan} \right]}{L^2} = \frac{P \cdot a}{6} - \frac{8 \cdot E \cdot I \cdot \Delta_{midspan}}{L^2} \quad (6)$$

The rotational stiffness can be calculated using Eqs. (2), (3) and (6) for test Type 6. The values are given in Table 3.

An average value of 40 kNm/rads is obtained from Table 3 for the rotational stiffness between the bearer and the pier connection.

5. Theoretical modelling

5.1 General

The floor to be modelled has bearers continuously over three spans of 3 metres and joists continuously over three spans of 1.8 metres. The overall dimensions of the floor are 9 metres by 5.4 metres. The joists are placed at 450 mm centres. The sizes for pier, bearer and joist are RHS 90 × 90 × 2, RHS 150 × 50 × 2 and RHS 100 × 50 × 2 mm respectively. The thickness of the particleboard is 19 mm.

The floor system was modelled as a grillage of beam elements, at varying levels of simplification. The structural analysis program SpaceGass (ITS 1998) was used. To develop a grillage model the particleboard had to be discretized. It was modelled as a series of beams spanning between the joists, and spaced at 300 mm centres. Each floor element therefore had the properties of a 300 mm wide piece of flooring.

5.2 Plane models (2D)

5.2.1 Model 1a

The simplest grillage model had all of the elements which comprise the floor system lying in one plane. The model, vibrating in its fundamental mode, is shown in Fig. 8. Please note that the same mode shape was achieved for all theoretical models. The mode is dominated by the motion of the bearers.

The calculated frequency for the fundamental mode is 18.62 Hz, which compares very well with the measured value of 18.9 Hz. This is encouraging, but also worrying as the model is not an accurate representation of the real structure, and therefore such good agreement should not be expected. The key features of this model are:

- all members lie in one plane, which is not the case in the actual floor
- the bending and shear stiffness of the joist/bearer connection is infinite
- the support stiffness of the post end connection is zero
- the composite joist/flooring member is modelled using the nominal value of the elastic modulus for the flooring material (3000 MPa)

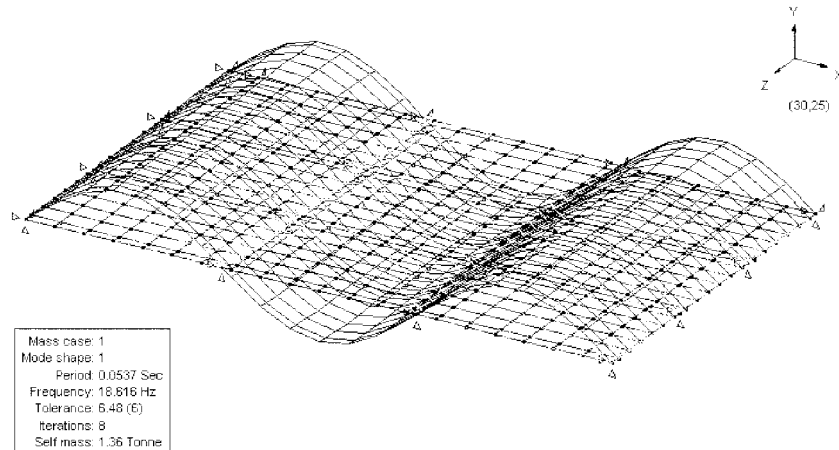


Fig. 8 Typical output of SpaceGass

5.2.2 Model 1b

This was the same as for model 1a, except that the effective elastic modulus for the flooring material (1,850 MPa, see Section 4.1) was used. The fundamental frequency changed only very slightly, to 18.600 Hz, indicating that partial shear connection between the joist and the flooring has no significant effect on the dynamic behaviour of the floor.

5.2.3 Model 1c and 1d

The lumped masses, representing 40 kg/m^2 and 90 kg/m^2 respectively along the bearers were added for model 1c and model 1d. As would be expected, the frequency of vibration decreased to 11.9 and 9.1 Hz respectively. The measured values were 22.2 and 22.8 Hz. This shows that the grillage model with all elements in one plane cannot simulate the behaviour of Stage 3 and Stage 4.

5.3 Multi-layer models (3D)

To represent the floor behaviour more accurately, a model was developed where each level of structure was represented at its centroid. Thus there was a vertical separation between the bearer elements and the joist elements, and a further separation between the joist elements and the flooring elements. The layers were connected at all nodes by vertical beam interface elements. As well as placing the structural elements in their correct physical location, and thereby introducing the additional stiffness achieved through the greater structural depth, this model allowed the influence of the bending and shear stiffness of the connections between the floor layers to be modelled by varying the properties of the interface elements that connected the layers together.

5.3.1 Model 2a

In the first of these models the bending and shear stiffness of the interface elements was made infinite that is complete shear connection was assumed. The fundamental frequency was 37.90 Hz, much greater than given by Model 1a, and much greater than the measured frequency (18.9 Hz).

5.3.2 Model 2b

The bending stiffness of the interface elements was reduced to give a rotational stiffness at the bearer to joist connection of 21.4 kNm/rad, in accordance with the results from the component tests. The fundamental frequency remained the same at 37.90 Hz, indicating that the bending stiffness of the bearer to joist connection has no significant effect on the dynamic behaviour of the floor.

5.3.3 Model 2c

Model 2b was now modified to include the measured rotational stiffness of 40 kNm/rad at the supports. The fundamental frequency changed slightly, to 38.16 Hz, indicating that the restraint offered by the supports has only a slight effect on the dynamic behaviour of the floor.

5.3.4 Model 2d

Next the shear stiffness of the interface element between the bearer and the joist was reduced to zero, which means that slip occurs at the interface. This implies that there is no shear restraints provided by bearers to joists. The fundamental frequency reduced to 19.3 Hz, or 18.62 Hz if the support restraint was ignored. As expected, the latter value is the same as obtained in Model 1a where all elements were in one plane, i.e., a two-dimensional model.

5.4 Results and discussions (Stage 1)

The results from the above Models are summarised in Fig. 9 where the measured frequency for stage 1 was also shown as a horizontal line. This figure highlights the findings from these models - that the partial shear connection between the joist and the flooring, the bending stiffness of the connection between the bearer and the joist, and the stiffness of the supports, have no significant effect on the frequency of the bare floor. However, the degree of shear connection between the bearer and the joist has a dramatic effect on the frequency of the floor vibration, and the bare floor (Stage 1) has negligible shear connection between these elements. It is clear from these results that the most effective way to increase the frequency of floor vibration for the bare floor situation is to improve the shear connection between the bearer and the joist.

The change in damping can also be explained by the change in shear connection. A significant source of damping is the slip that occurs between the joist and the bearer. The energy absorbed is a product of the shear force and the slip. As the lumped mass increases the shear force increases (because of the increased friction as described above), but the slip decreases. For Stage 1 the slip is

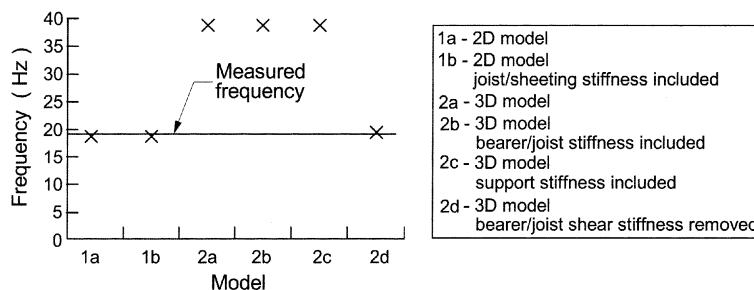


Fig. 9 Results of model types (Stage 1)

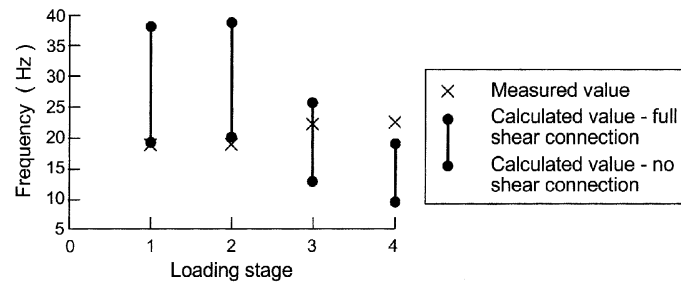


Fig. 10 Results of loading stages

high, but the shear force is approximately zero (no shear connection), so the damping from this source is low. At complete shear connection the slip is approximately zero, so the damping is low even though the shear force is high. With partial shear connection the damping from this source is maximised, as both the slip and the shear force are non zero.

5.5 Results and discussions (Stages 2, 3 and 4)

In the next models, construction stages 2, 3 and 4 were analysed, with and without shear connection between the bearer and the joist. Models 2c and 2d were used as the basis for these models. The walls (Stage 2) were modelled as vierendeel girders, assuming rigid joints between the studs and the top and bottom plate. The results of these analyses are presented in Fig. 10, together with the results from Stage 1.

The assumption of no shear connection at the joist to bearer connection gives good correlation with the measured frequency for the bare floor, and bare floor plus wall (Stages 1 and 2). However, when the lumped mass is included this assumption becomes increasingly inaccurate, and the behaviour moves towards that which is consistent with full shear connection. This is because the added mass increases the frictional force between the joist and the bearer, and so as the mass increases the degree of shear connection improves. From Fig. 10 it appears that Stage 4 (90 kg/m² added mass) has full shear connection, while at Stage 3 the shear connection is high but still partial. One of the methods to improve bearer-joist shear connection could be to apply some screws or nails at the far end connection between bearers and joists, or to apply glue between bearers and joists.

6. Conclusions

Based on the limited test results and theoretical analysis of DuraGal lightweight floor systems, the following observations and conclusions are made. It may not be applicable to other types of floors.

- The connection stiffness between different components in DuraGal lightweight floor systems has been obtained. Around 40% composite action was achieved between the RHS joist and the particleboard.
- The rotational stiffness between the joist and bearer has been found about 21.4 kNm/rads. The rotational stiffness between the bearer and pier has been found about 40 kNm/rads.
- The partial shear connection between the joist and the flooring, the bending stiffness of the connection between the bearer and the joist, and the stiffness of the supports, have no significant

effect on the frequency of the bare floor.

- The degree of shear connection between the bearer and the joist has a dramatic effect on the frequency of the floor vibration, and the bare floor (Stage 1) has negligible shear connection between these elements.
- The most effective way to increase the frequency of floor vibration for the bare floor situation is to improve the shear connection between the bearer and the joist.
- Increasing the mass of the walls and roof increases the frictional force between the joist and the bearer, which increases the shear connection between the joist and the flooring, so that the frequency of vibration can increase with the additional mass because of the increased stiffness of the floor system.

Acknowledgments

The authors are grateful to the Australian Research Council and BHP Steel Structural and Pipeline Products (now OneSteel Market Mills) for their financial support. Thanks are given to Mr. M. Lewis for conducting the component tests in the Civil Engineering Laboratory, Monash University.

References

- Alikhail, M., Zhao, X. L. and Koss, L. (1999), "Dynamic performance of steel lightweight floors", *Proc. 2nd Int. Conf. on Advances in Steel Structures*, Hong Kong, 849-856.
- Alikhail, M., Zhao, X.L., Koss, L., Dagg, H. and Shield, A. (1998), "High strength steel RHS, domestic flooring system", *Proc. Eighth Int. Symp. on Tubular Structures*, Singapore, 26-28 August, 635-173.
- Alikhail, M., Zhao, X.L. and Alisjahbana, S.W. (2000), "Dynamic properties of steel lightweight floors", *Int. Conf. on Advances in Structural Dynamic*, Hong Kong, 13-15, December.
- Alisjabana, S.W. (2000), "Response of large space building floors to dynamic loads which suddenly move to a new position", in *Structural Failure and Plasticity*, Zhao, X.L. and Grzebieta, R.H. (eds), Elsevier Science Ltd, 865-870.
- Alisjahbana, S.W., Zhao, X.L. and Alikhail, M.M. (2000), "Component of lightweight floor systems under human movement", *Int. Conf. on Advances in Structural Dynamic*, Hong Kong, 13-15 December.
- Alisjahbana, S.W. (1999), "Respons Dinamik Balok Teredam Akibat Beban Lateral Dinamik Yang Berpindah Secara Tiba-tiba di Arah Aksial", *Jurnal Teknik Sipil; Universitas Tarumanagara*, Jakarta, Indonesia, No. 3, Th. 5/1999, 229-243.
- Allen, D.E. and Rainer, J.H. (1976), "Vibration criteria for long span floors", *Canadian J. Civil Eng.*, **3**(2), 165-173.
- Couchman, G.H., Toma, A.M., Brekelmans, J.W.P.M. and Van den Brande, E.L. M.G. (1999), "Steel-board composite floors", in *Light-Weight Steel and Aluminium Structures*, Makelainen, P. and Hassinen, P. (eds), Elsevier, 317-324.
- Dawkins, D. and Cusack, D. (1993), *Australian Domestic Construction Manual*, Trevor Howse and Associates Pty Ltd and Quasar Management Services, NSW, Australia.
- ITS (1998), *Spacegass 8-Reference Manual*, Integrated Technical Software, Melbourne.
- Lenzen, K.H. (1966), "Vibration of steel joist-concrete slab floors", *AISC Eng. J.*, July 1966, 133-136.
- Murray, T.M. (1991), "Building floor vibration", *Engineering Journal/American Institute of Steel Construction*, Third Quarter/1991, 102-109.
- Ohlsson, S. (1982), "Floor vibration and human discomfort", PhD Thesis, Division of Steel and Timber Structures. Chalmers University of Technology, Goteberg Sweden.
- Onysko, D.M. (1995), "Some background on factors affecting performance of floors and setting of performance

- criteria”, Presentation to Task Group, Study on Serviceability Criteria for Floors, July, 1995.
- SAA (1980), *Flat Pressed Particleboard*, Australian Standard AS1859, Standard Australia, Homebush, NSW, Australia.
- Smith, I. and Chui, Y.H. (1988), “Design of lightweight wooden floors to avoid human discomfort”, *Can. J. Civil Eng.*, **15**, 254-262.
- Wiss, J.F. and Parmelee, R.A. (1974), “Human perception of transient vibration”, *J. Struct. Div.*, ASCE, **100**, April, 773-787.
- Zhao, X.L., Hancock, G.J. and Trahair, N.S. (1995), “Lateral buckling tests of cold-formed RHS beams”, *J. Struct. Engrg.*, ASCE, **121**(11), 1565-1573.
- Zhao, X.L. and Mahendran, M. (1998), “Recent innovation in cold-formed tubular sections”, *J. Constructional Steel Research*, **46**(1-3), paper 228.